Published in final edited form as:
Dev Biol. 2009 September 1; 333(1): 14–25. doi:10.1016/j.ydbio.2009.06.016.

Lmx1a maintains proper neurogenic, sensory, and nonsensory domains in the mammalian inner ear

Soo Kyung Koo[*,+], **Jennifer K. Hill**[*], **Chan Ho Hwang**, **ZhengShi Lin**, **Kathleen J. Millen**[#], and **Doris K. Wu**

National Institute on Deafness and Other Communication Disorders, 5 Research Court, Rockville MD, 20850, USA

[#]Department of Human Genetics, University of Chicago, Chicago, IL 60637, USA

Abstract

Lmx1a is a LIM homeodomain-containing transcription factor, which is required for the formation of multiple organs. *Lmx1a* is broadly expressed in early stages of the developing inner ear, but its expression is soon restricted to the non-sensory regions of the developing ear. In an Lmx1a functional null mutant, *dreher* (dr^J/dr^J), the inner ears lack a non-sensory structure, the endolymphatic duct, and the membranous labyrinth is poorly developed. These phenotypes are consistent with *Lmx1a*'s role as a selector gene. More importantly, while all three primary fates of the inner ear – neural, sensory, and non-sensory – are specified in dr^J/dr^J, normal boundaries among these tissues are often violated. For example, the neurogenic domain of the ear epithelium, from which cells delaminate to form the cochleovestibular ganglion, is expanded. Within the neurogenic domain, the demarcation between the vestibular and auditory neurogenic domains is most likely disrupted as well, based on the increased numbers of vestibular neuroblasts and ectopic expression of *Fgf3*, which normally is associated specifically with the vestibular neurogenic region. Furthermore, aberrant and ectopic sensory organs are observed; most striking among these is vestibular-like hair cells located in the cochlear duct.

Keywords

LIM homeodomain; inner ear development; Fgf3; transcription factor; neurogenic fate

Introduction

The formation of the mammalian inner ear requires a tightly regulated series of cell fate decisions and morphogenetic events, which converts a thickening of the ectoderm into a complex fluid-filled membranous labyrinth comprising one auditory and five vestibular organs. The organ of Corti within the mammalian cochlea responds to auditory stimuli. The vestibular organs mediating balance include, the cristae of the three semi-circular canals, which respond to angular acceleration, and the maculae of the utricle and saccule, which

Send Correspondence to: Doris K. Wu, Ph.D., 5 Research Court, Rm 2B34, Rockville, MD 20850, Tel: 301-402-4214, Fax: 301-402-5475, wud@nidcd.nih.gov.
[*]equal contribution
[+]Current address: Division of Cardiovascular and Rare Diseases, Center for Biomedical Sciences, National Institute of Health (NIH), Seoul, Republic of Korea

respond to linear acceleration. Maintaining the specific domains of sensory, non-sensory, and neuronal tissues that make up the intricate landscape of the inner ear is critical for the proper functioning of the auditory and vestibular systems. Complex cascades of signaling events undoubtedly direct the developmental processes that define and maintain these domains, but relatively few of the specific molecular components have been identified thus far (Anagnostopoulos, 2002; Kelley, 2006).

LIM homeodomain (LIM-hd) proteins are transcription factors critical to many cell fate decisions and patterning of organs (Hobert and Westphal, 2000). The two amino-terminal LIM motifs bind proteins and allow LIM-hd proteins to participate in heteromeric transcriptional complexes in a tissue-specific manner. The DNA-binding homeodomain is located towards the carboxy terminus of the protein. Conserved across phyla, LIM-hd proteins are divided into six major groups based on sequence homology. The vertebrate *Lmx* group has two paralogs: *Lmx1a* and *Lmx1b. Lmx1b* is identical to *Lmx1a* in its homeodomain; it is important for patterning of the limbs, calvarial bone, and chicken otic vesicles (Chen et al., 1998b; Giraldez, 1998; Riddle et al., 1995; Vogel et al., 1995). Mutations of *LMX1B* cause Nail Patella Syndrome (MIM #161200), a disorder characterized by defects in the limb, kidney, and eye (Chen et al., 1998a; Dreyer et al., 1998; Pressman et al., 2000). A developmental role for *Lmx1a* was implicated by analyses of *dreher* (dr^J/dr^J) mice, in which *Lmx1a* is mutated (Millonig et al., 2000). *Dreher* mice display a complex phenotype, including pigmentation anomalies and deafness, as well as abnormal development of the cerebellum, hippocampus, and cortex (Deol, 1964; Manzanares et al., 2000; Wahlsten et al., 1983). There is good evidence that *Lmx1a* functions as a selector gene in vertebrates (Chizhikov and Millen, 2004a; Millonig et al., 2000). For example, *Lmx1a* is expressed in the roof plate of the neural tube and this structure fails to develop in the absence of this gene product (Failli et al., 2002; Millonig et al., 2000). Moreover, ectopic expression of *Lmx1a* in chicken neural tubes induces roof plate formation (Chizhikov and Millen, 2004a).

Unlike many spontaneous mouse mutations that are represented by only one allele, there are eleven spontaneous *dr* mutant alleles, all of which display similar neurological, pigmentation, and skeletal defects. Ten of these alleles have been molecularly defined. The dr^J mutation, the best-studied allele, is a single G-to-A base pair mutation that alters a conserved cysteine, which is required for coordinating the binding of zinc essential for LIM domain function. dr^J/dr^J has a comparable phenotype to the four *dr* alleles that result in absence of protein suggesting that dr^J is a functionally null allele. Additionally, protein products resulting from dr^J cDNAs were unable to recapitulate exogenous wildtype Lmx1a activity when expressed in chicken (Chizhikov et al., 2006). Our phenotypic analyses of the *dreher* mutants corroborate a recent study showing *Lmx1a* is a key molecule in maintaining specified domains among sensory tissues within the inner ear (Nichols et al., 2008). Furthermore, our study demonstrates that *Lmx1a* is expressed early in development and influences specification of neural subtypes. We propose the sensory and neural defects may be related.

Materials and Methods

Mice and genotyping

Dreher^J heterozygous mice (Lmx1a$^{dr\text{-}J}$/J) were genotyped by PCR-restriction fragment length polymorphism using the following primers: 5’-AGCTTCTGGCACGAGCAAT and 5’-ACACCCGTGGAGGTGAGTG. The 154 bp PCR product from mutant mice is resistant to digestion by *HpyCH4V*, whereas amplicons from wildtype mice are digested.

Paint-fill, In situ hybridization, and Immunohistochemistry

In situ hybridization (ISH) and paint-filling of inner ears were performed as previously described (Morsli et al., 1998). Plasmids for generating *Lmx1a* and *Tlx3* riboprobes were gifts from Randy Johnson (Anderson Cancer Institute) and Quifu Ma (Harvard Medical School), respectively. Whole-mount specimens probed with *NeuroD* were blind-scored by two investigators. Three-dimensional reconstructions of serial cryosectons of two pairs of wildtype and mutant inner ears after ISH were generated using ROSS software (Biocomputation Center, Ames Research Center, NASA). Only the outlines of the inner ear lumen and expression domains of various genes were traced for reconstruction. Two additional pairs of wildtype and mutant ears were partially reconstructed to measure the CVG area. *NeuroD* positive regions of the CVG in each section were circled and the area calculated using ROSS software. The areas were summed and reported as mean $\mu m^2 \pm$ SEM.

Whole-mount cochlear ducts were fixed with 4% formaldehyde overnight at 4°C before further dissection and labeling. Tissues were incubated with anti-P75Ngfr (1:1000; Chemicon) or anti-2H3 (anti-neurofilament; 1:200; Developmental Studies Hybridoma Bank) followed by anti-rabbit IgG Alexa568 (1:200; Invitrogen) or anti-mouse IgG Alexa680 (1:200; Invitrogen). All tissues were co-labeled with FITC-phalloidin (1:40; Invitrogen).

Results

Morphogenetic malformations and larger cochleovestibular ganglion in *dreher* inner ears

We investigated the role of *Lmx1a* in inner ear formation by analyzing the paint-filled inner ears of *dreher* mutants. At 11.5 days post coitum (dpc), inner ears of dr^J/dr^J mutants show a lack of endolymphatic duct (ED) and retarded development of semicircular canals and the cochlear duct (Fig. 1A,B). Between 11.5 to 15.5 dpc, normal inner ears undergo a remarkable degree of growth and morphogenesis, and their gross anatomy is nearly mature by 15.5 dpc (Fig. 1A,C). In contrast, at this age, the anatomy of dr^J/dr^J inner ears appears arrested at an earlier stage of development (Fig. 1D; n=6). Notably, in mutants there is no resorption of the epithelium in the canal pouches, which is required for normal canal formation, and only a partial extension of the cochlear duct. The ED fails to form and only a slight evagination is present in place of a saccule (Fig. 1D, asterisk). These abnormalities do not improve by birth and are consistent with what were described over 40 years ago (Deol, 1964). Furthermore, the cochleovestibular ganglia (CVG) in dr^J/dr^J appear to be larger in size than those in $dr^J/+$ (Fig. 1E,F; white outline, 9.5-10.5 dpc, n=3/4).

Abnormal sensory organ development in dr^J/dr^J mutants

Next, we asked whether all the sensory organs are present within the rudimentary membranous chamber of dr^J/dr^J mutants. Whole-mount phalloidin labeling of the dissected membranous portion of dr^J/dr^J inner ears indicate that all six sensory organs, which include three cristae, two maculae, and the organ of Corti, are present at 18.5 dpc (Fig. 2A,B; n=13). These data are consistent with previous studies using *Atoh1* or *Bdnf-LacZ* as a marker for inner-ear sensory epithelia (Matei et al., 2005). Additionally, ectopic sensory patches containing sensory hair cells can be found adjacent to the maculae of the utricle and saccule (Fig. 2C-E; n=4). Based on hair bundle morphology we conclude that these ectopic sensory patches have vestibular-like hair cells. The cochlear duct is shortened and lacks pillar cell-associated p75Ngfr labeling in the basal region (Fig. 2C,F; n=4). Additionally, based on the morphology of the apical hair bundles, hair cells in the basal cochlea more closely resemble hair cells found in a normal macula than those in the organ of Corti (Fig. 2F,G). Similar findings have been reported recently (Nichols et al., 2008). However, this apparent

phenotypic conversion is incomplete. Based on anti-neurofilament labeling, no organized calyxes are found surrounding these cells as those in a normal macula (Fig. 2F,G). In the mid to apical region of the cochlear duct, normal rows of hair cells are present, separated by a row of p75Ngfr-positive pillar cells (Fig. 2H,I).

Normally, the anterior and posterior cristae are structurally indistinguishable from each other; each consists of two equal halves of sensory tissue bisected by a non-sensory structure, the cruciatum (Fig. 2M; arrow). In contrast, the cristae of dr^J/dr^J mutants are often malformed. The posterior cristae of dr^J/dr^J mutants show a range of malformations (Fig. 2C,N,O; n=6/6); in one mutant posterior crista, two cruciatum-like structures were found adjacent to each other (Fig. 2N, double arrows). The anterior and lateral cristae are normally distinct entities, however in dr^J/dr^J mutants they are sometimes fused (Fig. 2K, compare to J; n=3/6), and the two halves of the anterior crista are often asymmetric with the medial half larger than the lateral half (Fig. 2C,L,M; n=5/6). Despite these gross malformations, hair cells within all three cristae appear normal, as evidenced by hair bundle patterns and calyxes surrounding the hair cell bodies (Fig. 2P).

Lmx1a expression subdivides neurogenic domains of the otocyst and influences neural subtype specification

Lmx1a is expressed throughout the otic placode, but its expression is soon restricted to specific regions of the otocyst (Failli et al., 2002). We find that *Lmx1a* expression in the ear has a dynamic spatiotemporal pattern through 13.5 dpc. To better understand the cause of the neural and sensory phenotypes in dr^J/dr^J mutants, we compared the normal expression pattern of *Lmx1a* with other genes that are expressed in all or part of the neurogenic domain, such as *NeuroD, Gata3*, and *Fgf3*.

NeuroD expression serves as a proxy for the entire neurogenic region, since all otic neuroblasts presumably express this gene prior to and shortly after their delamination (Lawoko-Kerali et al., 2004; Liu et al., 2000). During otocyst stages, the *Lmx1a* expression subdivides the *NeuroD*-positive domain within the otic epithelium. Whole-mount ISH of 9.5 dpc otocysts shows *Lmx1a* is not expressed in the lateral region of the neurogenic domain (Fig. 3A; arrowheads). A more detailed 3D-reconstruction of a cryosectioned otocyst at 10.5 dpc probed for *Lmx1a* (Fig. 3B,C, pink) and *NeuroD* (Fig. 3B,C, yellow) transcripts indicates that while the lateral neurogenic region is devoid of *Lmx1a* expression, a majority of the neurogenic region on the medial side is within the domain of *Lmx1a* expression. Despite this overlap on the medial side, there is a small ventral-medial neurogenic region of the otocyst that does not show *Lmx1a* expression (Fig. 3C, asterisk; 3F,G; arrowheads). Interestingly, previous studies demonstrated that the lateral-medial axis of the neurogenic region encodes information pertaining to neuronal subtype specification, with vestibular neuroblasts delaminating from the lateral region of the neurogenic domain and auditory neuroblasts originating from the medial region, which selectively expresses *Gata3* (Lawoko-Kerali et al., 2004). Adjacent sections comparable to those shown in Figs 3D and E indicate *Lmx1a* and *Gata3* are co-expressed in this medial neurogenic region (Fig. 3H,I). While further fate mapping data are required to verify whether the *Gata3*-positive neurogenic region is exclusively auditory, our data, taken at face value, suggest *Lmx1a* is expressed in the *Gata3*-positive, auditory region (Fig. 3D,E,H,I brackets) but not the vestibular neurogenic region (Fig. 3D,E; arrowheads) of the developing inner ear. This result, together with the increased in size of dr^J/dr^J CVG led us to hypothesize that *Lmx1a* plays a role in specifying distinct neuronal subtypes during ear development.

To test this hypothesis, we first analyzed in greater detail the CVG of dr^J/dr^J mutants between the ages of 10.5 (n=11) and 11.5 dpc (n=5). Three-dimensional reconstruction of otocysts at 10.5 dpc indicated the epithelial *NeuroD* expression domain (Fig. 4A, red) is

expanded in dr^J/dr^J mutants compared to $dr^J/+$, particularly on the medial side (Fig. 4C, asterisk; 4G,K; bracket). Consistent with whole-mount ISH results (Fig. 1), we find the total area of the dr^J/dr^J CVG (3449±425 μm^2; n=4) to be larger than that of wildtype (2287±169 μm^2; n=4; $p< 0.05$; Fig. 4A-D, yellow). Vestibular neuroblasts are thought to be *Tlx3* positive (Zopf et al., 2007), and are located dorsal to the auditory neuroblasts in the CVG (Fig. 4B, green; Fig. 4E,F). In dr^J/dr^J inner ears, there is a ventral (Fig. 4D,L) expansion of the *Tlx3*-positive region as well as a subtle but consistently larger region of *Tlx3* positive neuroblasts in comparison to $dr^J/+$ specimens (Fig. 4F,H,J,L; arrowheads). Furthermore, some *Tlx3* positive cells are found in the most ventral region of the CVG (Fig. 4D), whereas there are none at that level in heterozygous ears (Fig. 4B).

Although we see a ventral expansion of *Tlx3* expression in the CVG of dr^J/dr^J mutants, there is no obvious change in the *Gata3* expression domain in the CVG of dr^J/dr^J mutants compared to $dr^J/+$ littermates at 10.5 dpc (Fig. S3). Within the otic epithelium, there is no expansion of *Gata3* expression into the vestibular neurogenic region (Fig. 5B,D; arrowheads). On the medial side where *NeuroD* expression is expanded in dr^J/dr^J mutants, it is unclear whether *Gata3* expression is also upregulated or expanded since that region is normally *Gata3* positive (Fig. 5A-D; bracket). Furthermore, the relationships between *Lmx1a* and *Gata3* expression domains in dr^J/dr^J mutants are also comparable to that of the wildtype. (Fig. 5E-H). Similar expression patterns of *Tlx3* and *Gata3* in the CVG and otic epithelium of dr^J/dr^J mutants are evident at 11.5 dpc (Fig. S4). These results suggest that there is an increase in the number of vestibular neuroblasts but no obvious change in auditory neuroblasts in dr^J/dr^J mutants compared to controls.

Since *Tlx3* expression is detected only after neuroblasts have delaminated from the epithelium (Fig. 4E-L), we sought a marker of the antero-ventral-lateral otocyst that overlaps with *NeuroD* expression only in the presumptive site of origin for vestibular neurons. Currently, the best candidate for such a marker is *Fgf3*, which is expressed in the neurogenic region devoid of *Lmx1a* (Fig. 6A,B). *Fgf3* expression also persists in some of the neuroblasts that delaminate from this region (Fig. 6B; arrows; (McKay et al., 1996)). *Fgf3* knockout mice show a reduction in the size of the CVG, although no specific role in vestibular ganglion formation has yet been proposed for this gene (Hatch et al., 2007; Mansour et al., 1993). We examined whether the *Fgf3* expression domain is affected in dr^J/dr^J mutants. Dorsally, *Fgf3* expression patterns of dr^J/dr^J and $dr^J/+$ mice are indistinguishable, except that there are generally more delaminated *Lmx1a*-labeled cells in dr^J/dr^J mutants (Fig. 6C; arrows). However, in the ventral otocyst of dr^J/dr^J mutants, there is an abnormal medial expansion of the *Fgf3* domain compared to $dr^J/+$ (Fig. 6E-L; arrows; n=3). These results support the notion that the otic epithelial region specified to form vestibular neuroblasts is indeed expanded in mutants, even though there is no obvious change in the size of the *Gata3*-positive auditory ganglion (Fig. 5, S3). By 15.5 dpc, the size of the vestibular ganglion in dr^J/dr^J mutants is small indicating that many of the vestibular neuroblasts do not survive subsequently, possibly due to the mis-specification of the vestibular neurogenic fate or lack of trophic support from the malformed vestibular sensory organs, or both (data not shown).

Lmx1a inner ear expression is restricted over time to non-sensory structures

After neuroblasts delaminate to form the CVG, the remaining cells in the neurogenic region are thought to give rise to two of the six sensory organs within the inner ear, the maculae of the utricle and saccule (Koundakjian et al., 2007; Raft et al., 2007). To date, there is no direct evidence that the prosensory regions of the cochlea (the organ of Corti) and cristae, originate within the neurogenic domain (Koundakjian et al., 2007; Raft et al., 2007). The *Lfng* expression domain, which includes but is broader than that of *NeuroD*, is thought to encompass the prospective organ of Corti and the two maculae (Fig. S1; (Fekete and Wu,

2002; Morsli et al., 1998)). Even though the precise locations of individual presumptive sensory organs cannot be distinguished easily within the *Lfng* or *NeuroD* domain at early stages, the broad overlap between *Lfng/NeuroD* and *Lmx1a* positive regions suggests that at least some prospective sensory organs are located within the *Lmx1a* domain (Figs. 3,S1). However by 13.5 dpc, when each sensory patch can be identified, *Lmx1a* expression is absent from the sensory structures and present only in adjacent non-sensory regions (data not shown).

The three presumptive cristae are initially demarcated by the expression of *Bmp4*, adjacent to the *Lfng/NeuroD* domain (Chang et al., 2003; Morsli et al., 1998). At 10 dpc, *Lmx1a* is not expressed in the developing lateral crista. In contrast, *Lmx1a* is expressed in the *Bmp4*-positive, presumptive posterior crista (Fig. 3J,K; arrows), and its expression partially overlaps with the prospective anterior crista. However, as in the maculae and organ of Corti, *Lmx1a* expression is downregulated in the differentiating cristae by E11.5 and ultimately absent from the mature sensory structures (data not shown).

The anatomy of the inner ear is more distinct by 15.5 dpc. At this stage, *Lmx1a* is expressed only in non-sensory regions of the inner ear such as the ED, transitional zones of cristae, the roof of the maculae utricle and saccule, and parts of the cochlea including the Reissner's membrane and stria vascularis (Fig. S2). As described above, none of the anatomically differentiated sensory organs express *Lmx1a*. A similar pattern of *Lmx1a* expression in non-sensory regions of the inner ear has been described elsewhere (Huang et al., 2008). In dr^J/dr^J mutants, while the membranous labyrinth is enlarged and amorphic at 15.5 dpc, the *Lmx1a* positive regions remain non-overlapping with the sensory domains (data not shown).

Abnormal gene expression in the cochlea and cristae of dr^J/dr^J mutants

We have found that sensory hair cells in the basal region of the dr^J/dr^J cochlear duct have some characteristics of vestibular hair cells (Fig. 2F). To further explore this phenotype, we looked at the expression of genes that distinguish between developing vestibular and auditory hair cells. *Fgf8* is normally expressed in all hair cells of the vestibular organs but only in inner hair cells of the organ of Corti (Fig. 7A,A'; arrowheads and arrow). At 16.5 dpc, *Pax2* is expressed strongly in all vestibular hair cells, but is barely detectable in cochlear hair cells (Fig. 7B,B'; arrowheads and short arrow). These expression patterns are maintained in the dr^J/dr^J cochlea from mid- to apical regions; *Fgf8* is expressed by inner hair cells (Fig. 7C,C') and *Pax2* expression is undetectable (Fig. 7D,D'; short arrow). However, in the basal region of the mutant cochlea, large numbers of *Fgf8* and *Pax2* positive hair cells are present (Fig. 7E,F,H,I), indicating that these cells have a gene expression profile normally associated with vestibular hair cells. Interestingly, these dr^J/dr^J cells develop in a cochlear territory that is innervated by spiral ganglion and maintains expression of other cochlear-specific sensory genes, such as *Gata3* (Fig. 7G;(Nichols et al., 2008)).

Pax2 expression in the abneural cochlear duct includes the developing stria vascularis, a non-sensory structure responsible for maintaining fluid homeostasis (Burton et al., 2004). While the mid and apical regions of the dr^J/dr^J organ of Corti appears to develop normally, abneural *Pax2* expression is absent along the entire length of the cochlea (Fig. 7B,D, long arrow). *Trp2*, which is expressed in neural crest-derived melanocytes within the stria vascularis (Steel et al., 1992), is also absent. Additionally, the formation of another *Lmx1a*-positive non-sensory cochlear structure, the Reissner's membrane (Fig. S2), is affected in dr^J/dr^J as well based on *Otx2* expression not being consistently found in all sections of the cochlear duct (Fig. 7L,M). Together, these results suggest that *Lmx1a* is required for proper development of the non-sensory region of the cochlear duct.

Gene expression analyses also revealed an early basis for the observed crista defects. For example, three out of four mutant specimens showed an abnormal medial expansion of *Bmp4* expression in the presumptive anterior crista by 11.5 dpc (Fig. 7N,O; arrows). This finding is consistent with a broader medial half of the anterior crista frequently observed in mutants at later stages (Fig. 2C,L).

Dlx5, a dorsal otic marker, is expanded in dr^J/dr^J mutants

In a normal inner ear, vestibular sensory organs are located dorsal to the organ of Corti. The presence of vestibular-like sensory tissues in the cochlear region and expansion of the vestibular neurogenic domain ventrally in dr^J/dr^J mutants could represent a problem in axial specification of the inner ear, resulting in an expansion of dorsal fates and/or loss of ventral fates. We therefore examined the expression patterns of *Dlx5* and *Otx1*, which are differentially expressed along the dorso-ventral axis of the otocyst (Merlo et al., 2002; Morsli et al., 1999). *Dlx5* is a robust dorsal marker, expressed in the ED (Fig. 8A; arrow) and canal pouches of the developing otocyst, but absent in the primordial cochlear duct (Fig. 8C; arrowheads). Despite a smaller canal pouch in dr^J/dr^J mutants, *Dlx5* expression is similar to that in dr^J/+ inner ears (Fig. 8B; arrow). However, the domain of *Dlx5* was found to extend ventrally into the cochlear duct region in dr^J/dr^J mutants, a pattern never observed in dr^J/+ inner ears (Fig. 8C,D; arrowheads; n=8). The abnormal expansion of the *Dlx5* expression domain remains at 16.5 dpc (data not shown) in dr^J/dr^J. Conversely, we did not find the domain of *Otx1*, which is specifically expressed in the ventral otocyst and cochlear duct (Morsli et al., 1999), to be abnormally patterned along the dorso-ventral axis of dr^J/dr^J otocysts (n=2, data not shown).

Lmx1a acts independently of *Gbx2* in endolymphatic duct formation

The ED, which normally expresses *Lmx1a*, fails to develop in dr^J/dr^J mutants (Figs 1,3,S2). *Gbx2* is another known gene that is required for ED formation, and the lack of *Gbx2* indirectly affects *Wnt2b* expression in this structure (Lin et al., 2005). Thus, we investigated whether *Lmx1a* mediates ED formation via *Gbx2* and/or *Wnt2b*. At 10.5 dpc, the base of the developing ED in dr^J/+ otocysts is *Gbx2* and *Wnt2b* positive (Fig. 9A,B). At a comparable region of dr^J/dr^J otocysts, there is a small notch that resembles the ED rudiment; this notch is *Gbx2* positive but *Wnt2b* negative (Fig. 9C,D; arrows; n=8). By 11.5 dpc, *Gbx2* expression is no longer detectable in dr^J/dr^J embryos (data not shown). These results indicate that the rudimentary ED that fails to develop in dr^J/dr^J inner ears initially expresses *Gbx2* but not *Wnt2b*; furthermore, this rudimentary duct is *Dlx5* positive (Fig. 8B; arrowhead, n=4).

To gain further insight into the relationships between *Lmx1a* and *Gbx2* in ED formation, we examined the expression of *Lmx1a* in *Gbx2-/-* mutants. We found that *Lmx1a* is expressed in the medial region of the otocyst in *Gbx2-/-* embryos (Fig. 9E,F; arrow, n=2). Together, these results suggest that *Lmx1a* and *Gbx2* independently regulate ED formation.

Discussion

Lmx1a maintains tissue boundaries

Selector proteins are transcription factors required for the formation of specific body regions, organs, tissues, and cell types (Mann and Carroll, 2002). These proteins mediate a complex hierarchy of gene interactions, which confer affinities among cells in a given region and specification of one or more cell types within a defined compartment. Some of these functions are well illustrated in studies of the gene *apterous (ap)*, which encodes a LIM-hd protein required for *Drosophila* wing formation (Diaz-Benjumea and Cohen, 1993; Milan and Cohen, 1999; Milan and Cohen, 2003). *Apterous* is exclusively expressed in the

dorsal region of the wing imaginal disc, and wings fail to develop in the absence of *ap* (Cohen et al., 1992; Williams et al., 1993). Clonal analyses of *ap* negative cells within a wildtype imaginal disc revealed specific roles of ap in mediating cell affinities and boundary formation. In *ap* deficient clones, dorsal cells migrate to the ventral side and develop ventral identity. An ectopic wing margin forms when *ap* negative clones are juxtaposed to wildtype dorsal cells. Moreover, ventral cells ectopically expressing *ap* cross this normally tightly regulated border and express dorsal genes.

Two vertebrate LIM-hd proteins, *Lmx1a* and its paralog *Lmx1b*, demonstrated similar selector functions in roof plate and dorsal limb bud formation, respectively (Chen et al., 1998a; Millonig et al., 2000). While gene expression pattern and fate-mapping studies support a role of *Lmx1b* in border formation in the limb bud, direct experimental evidence is lacking (Arques et al., 2007; Pearse et al., 2007). Our phenotypic analyses of *dreher* mutants indicate that *Lmx1a*'s main function in the inner ear is to maintain the specified domains between regions with distinct developmental fates. Although the lack of both an ED and proper ear morphogenesis are phenotypes consistent with *Lmx1a* functioning as a selector gene, it is not required for the induction or specification of the three primary fates of inner ear tissues – neural, sensory, and non-sensory. Instead, it is required for the proper segregation of these distinct domains, since lack of functional Lmx1a causes: 1) expansion of the neurogenic area, 2) an abnormal boundary between vestibular and auditory neurogenic domains, and 3) abnormal size and shape of individual sensory organs. The mechanisms underlying aberrant boundaries in dr^J/dr^J inner ears are not clear. Lmx1a could normally suppress the vestibular neurogenic fate by negatively regulating *Fgf3*. Alternatively, the ectopic *Fgf3* expression could be a result of abnormal cell movements across an otherwise established boundary. Nevertheless, the similarity in *Lmx1a* expression domains between wildtype and dr^J/dr^J inner ears is evidence that there is not much cell movement out of the *Lmx1a* domain in the mutant (Fig. 6).

Neurogenic defects in dr^J/dr^J mutants

Neuroblasts initially delaminate from the otic epithelium to form the CVG, which later splits to form the vestibular and auditory ganglion. However, two lines of evidence suggest that the vestibular and auditory fates are established early before neuroblasts leave the otic epithelium. First, gene expression analyses suggest that vestibular and auditory neuroblasts originate from different regions of the otocyst; *Gata3*-negative vestibular neuroblasts delaminate from the lateral region whereas *Gata3*-positive auditory neuroblasts delaminate from the medial neurogenic region (Lawoko-Kerali et al., 2004). Second, more recent fate mapping studies suggest that the vestibular neuroblasts depart from the otic epithelium slightly earlier than neuroblasts destined to form the auditory ganglion (Bell et al., 2008; Koundakjian et al., 2007). Here, we show that *Lmx1a*, which is expressed in the *Gata3*-positive neurogenic region, functions to maintain a boundary between the presumed vestibular and auditory neurogenic regions (Fig. 10). In the absence of *Lmx1a*, the expression of a vestibular neurogenic marker, *Fgf3*, is expanded medially into the putative auditory neurogenic domain and an increased number of *Tlx3*-positive, vestibular neuroblasts is observed.

Is the sensory defect in dr^J/dr^J cochlear duct a result of abnormal DV axial specification?

The most striking sensory defect in dr^J/dr^J mutants is the presence of hair cells with vestibular characteristics in the basal region of the cochlear duct. Secreted molecules such as Wnts and Bmps originating from the dorsal neural tube and Sonic hedgehog (Shh) originating in the ventral neural tube and notochord, are thought to be important for establishing the DV axis of the inner ear (Bok et al., 2007a; Riccomagno et al., 2002; Riccomagno et al., 2005). Since vestibular hair cells are positioned dorsal to the auditory

hair cells in the normal mammalian inner ear, the expansion of vestibular hair cells into the cochlear duct of dr^J/dr^J mutants could be considered part of a dorsalized phenotype. Interestingly, ectopic vestibular-like sensory cells outside of the organ of Corti have been reported in mouse models with reduced ventral signaling via Shh (Driver et al., 2008). Too much Wnt signaling also causes the formation of vestibular-like hair cells in the basila papilla (cochlear duct) of chicken (Stevens et al., 2003).

The expansion of a bona fide dorsal marker, *Dlx5*, into ventral dr^J/dr^J otocysts does support the notion that that the mutant ears may be dorsalized. Whether the ventral expansion of *Dlx5* expression is directly related to the sensory or neurogenic phenotype is not clear since *Dlx5* is largely excluded from the neural-sensory domain in both wildtype and mutant otocysts (data not shown). A dorsalized inner ear could also result from reduced ventral signaling. However, ventral identity appears normal in dr^J/dr^J mutants, based on the presence of some of the ventral inner ear genes such as *Otx2* and *Msx1* (Fig. 7; data not shown; (Bok et al., 2007a; Bok et al., 2007b)).

Neural and sensory defects in *Dreher* mutants may be related

The normal expression pattern of *Lmx1a* bordering each sensory organ as well as the sensory organ defects observed in *dreher* mutants, support a role for *Lmx1a* in mediating directly the final shape and size of the sensory organ. Additionally, it is also possible that some of the sensory defects observed in *dreher* mutants are related to the earlier neurogenic defects since neuroblasts, sensory hair cells, and supporting cells are lineage related (Koundakjian et al., 2007; Raft et al., 2007; Satoh and Fekete, 2003). Under such a scenario, the ectopic sensory organs within the amorphic membranous labyrinth could be a consequence of the expanded neurogenic domain. To further expand on this idea, it is also possible that within a given lineage, the choice of neuroblasts and the type of sensory organ that develops subsequently are related. Thus, the hair cell phenotype in the basal cochlear duct is related to the fate change observed in the neuroblasts. When some of the cells within the auditory neurogenic region of dr^J/dr^J aberrantly took on a vestibular neurogenic fate as determined by *Tlx3* expression, the fate of lineage-related cells that remained in the epithelium could also be altered and obligated to form vestibular hair cells. This hypothesis remains to be tested.

Endolymphatic duct formation and inner ear morphogenesis

The ED, which is essential for maintaining fluid homeostasis in the mature inner ear, is the first structure to emerge from the rudimentary otocyst (Everett et al., 2001; Karet et al., 1999; Morsli et al., 1998). Our results identify *Lmx1a* as a required gene for ED formation. Moreover, we present data to suggest that *Lmx1a* functions independently of *Gbx2*, another gene required for ED formation. Gbx2 regulates the expression patterns of *Dlx5* and *Wnt2b* in the ED, although the effect of *Gbx2* on *Wnt2b* is thought to be indirect (Lin et al., 2005). In contrast, *Lmx1a* regulates the expression of *Wnt2b* and not that of *Dlx5* in the rudimentary ED (Figs. 8D,7B). Although there appears to be a slight down-regulation of *Gbx2* in the dr^J/dr^J mutants, the effect is not comparable to the downregulaton of *Wnt2b* observed and it could be due to a reduction in cell number. Therefore, a lack of identifiable cross-regulation between *Gbx2* and *Lmx1a* further suggests that these two genes mediate separate pathways in ED formation.

Several lines of indirect evidence suggest that the inner ear defects observed in the dr^J/dr^J mutants are primarily due to loss of *Lmx1a* within the otic epithelium rather than the hindbrain. First, the neural and sensory phenotypes in dr^J/dr^J inner ears indicate an expansion of dorsal fates. A ventralized rather than a dorsalized inner ear would be more in line with the reported absence of the roof plate in the hindbrain, which should reduce the

signals that are required to dorsalize the inner ear (Millen et al., 2004; Riccomagno et al., 2005). Second, the failure of ED formation in *kreisler* mutants has been attributed to defects in the hindbrain. While the downstream pathways of *Mafb* (the gene disrupted in *kreisler*) are not clear, one of the main consequences of the hindbrain defects is thought to be the loss of *Gbx2* expression in the inner ear (Choo et al., 2006). When *Wnt1* and *Wnt3a* are both knocked out in the hindbrain, *Gbx2* expression in the inner ear is absent as well (Riccomagno et al., 2005). In dr^J/dr^J inner ears, however, *Gbx2* expression is relatively normal, implying that the affected pathways in the hindbrain of some of these established mutants are most likely intact in dr^J/dr^J mice. Although extensive gene expression analyses in the hindbrain have not been done, our results support a minimal involvement of the hindbrain in contributing to defects in dr^J/dr^J inner ears. This hypothesis will be tested with tissue specific knockouts of *Lmx1a*, which are currently underway.

Our gene expression analyses indicate that most of the known genes required for inner ear morphogenesis are either normal or initiated normally in dr^J/dr^J inner ears. For example, *Netrin1* and *Nor-1*, which are important for proper canal resorption (Ponnio et al., 2002; Salminen et al., 2000), show normal expression patterns in the rudimentary canal pouch of dr^J/dr^J inner ears (data not shown). In addition, the early expression of *Pax2* in dr^J/dr^J otocysts is not markedly changed (data not shown), even though it is not expressed later in the cochlear duct. Thus, genes regulated by Lmx1a in the inner ear remain elusive. In the hindbrain, Lmx1a has been shown to act at the intersection of multiple signaling pathways, each of which is regulated by multiple redundant molecules. When individual genes upstream and downstream of *Lmx1a* such as the *Bmps* and *Wnts*, are mutated in the roof plate, a *dreher*-like phenotype is not recapitulated (Chizhikov and Millen, 2004b). Nevertheless, these molecules are dysregulated in the absence of functional Lmx1a. Similar to the hindbrain, Lmx1a could be interacting with multiple signaling pathways within the inner ear. Additionally, induction of the *Drosophila* wing margin by *apterous* involves regulating components of the Notch signaling pathway such as serrate, delta, and fringe (Milan and Cohen, 1999; Milan and Cohen, 2003). Most of these molecules have well-established roles in sensory organ and cell type specification in the inner ear (Kelley, 2006). Whether Lmx1a regulates the Notch signaling pathway in the inner ear is not clear. Therefore, future investigations will focus on the molecular pathways underlying Lmx1a's function as a selector gene in inner ear development.

Supplementary Material

Refer to Web version on PubMed Central for supplementary material.

Acknowledgments

We thank Matthew Chang and Lydia Lui for generating the 3-D images, Brad Buran for contributing to *Lmx1a* expression study, Anne Lindgren and Yuriko Mishima for assistance with embryo collection, and Drs. Quifu Ma and Randy Johnson for riboprobes. We appreciate Drs. Bernd Fritzsch, David Nichols, and Zheng-Yi Chan sharing their results prior to publication. We also thank members of the Wu lab and Drs. Thomas Friedman and Robert Morell for their insightful comments. K.J.M supported by NIH R01 NS044262

References

Anagnostopoulos AV. A compendium of mouse knockouts with inner ear defects. Trends Genet. 2002; 18:499. [PubMed: 12350347]

Arques CG, Doohan R, Sharpe J, Torres M. Cell tracing reveals a dorsoventral lineage restriction plane in the mouse limb bud mesenchyme. Development. 2007; 134:3713–22. [PubMed: 17715176]

Bell D, Streit A, Gorospe I, Varela-Nieto I, Alsina B, Giraldez F. Spatial and temporal segregation of auditory and vestibular neurons in the otic placode. Dev Biol. 2008; 322:109–20. [PubMed: 18674529]

Bok J, Chang W, Wu DK. Patterning and morphogenesis of the vertebrate inner ear. Int J Dev Biol. 2007a; 51:521–33. [PubMed: 17891714]

Bok J, Dolson DK, Hill P, Ruther U, Epstein DJ, Wu DK. Opposing gradients of Gli repressor and activators mediate Shh signaling along the dorsoventral axis of the inner ear. Development. 2007b; 134:1713–22. [PubMed: 17395647]

Burton Q, Cole LK, Mulheisen M, Chang W, Wu DK. The role of Pax2 in mouse inner ear development. Dev Biol. 2004; 272:161–75. [PubMed: 15242798]

Chang, W.; Cole, LK.; Cantos, R.; Wu, DK., editors. Molecular Genetics of vestibular organ development. Springer-Verlag; New York: 2003.

Chen H, Lun Y, Ovchinnikov D, Kokubo H, Oberg KC, Pepicelli CV, Gan L, Lee B, Johnson RL. Limb and kidney defects in Lmx1b mutant mice suggest an involvement of LMX1B in human nail patella syndrome. Nat Genet. 1998a; 19:51–5. [PubMed: 9590288]

Chen H, Ovchinnikov D, Pressman CL, Aulehla A, Lun Y, Johnson RL. Multiple calvarial defects in lmx1b mutant mice. Dev Genet. 1998b; 22:314–20. [PubMed: 9664684]

Chizhikov V, Steshina E, Roberts R, Ilkin Y, Washburn L, Millen KJ. Molecular definition of an allelic series of mutations disrupting the mouse Lmx1a (dreher) gene. Mamm Genome. 2006; 17:1025–32. [PubMed: 17019651]

Chizhikov VV, Millen KJ. Control of roof plate formation by Lmx1a in the developing spinal cord. Development. 2004a; 131:2693–705. [PubMed: 15148302]

Chizhikov VV, Millen KJ. Mechanisms of roof plate formation in the vertebrate CNS. Nat Rev Neurosci. 2004b; 5:808–12. [PubMed: 15378040]

Choo D, Ward J, Reece A, Dou H, Lin Z, Greinwald J. Molecular mechanisms underlying inner ear patterning defects in kreisler mutants. Dev Biol. 2006; 289:308–17. [PubMed: 16325169]

Cohen B, McGuffin ME, Pfeifle C, Segal D, Cohen SM. apterous, a gene required for imaginal disc development in Drosophila encodes a member of the LIM family of developmental regulatory proteins. Genes Dev. 1992; 6:715–29. [PubMed: 1349545]

Deol MS. The Origin of the Abnormalities of the Inner Ear in Dreher Mice. J Embryol Exp Morphol. 1964; 12:727–33. [PubMed: 14251482]

Diaz-Benjumea FJ, Cohen SM. Interaction between Dorsal and Ventral Cells in the Imaginal Disc Directs Wing Development in Drosophila. Cell. 1993; 75:741–752. [PubMed: 8242746]

Dreyer SD, Zhou G, Baldini A, Winterpacht A, Zabel B, Cole W, Johnson RL, Lee B. Mutations in LMX1B cause abnormal skeletal patterning and renal dysplasia in nail patella syndrome. Nat Genet. 1998; 19:47–50. [PubMed: 9590287]

Driver EC, Pryor SP, Hill P, Turner J, Ruther U, Biesecker LG, Griffith AJ, Kelley MW. Hedgehog signaling regulates sensory cell formation and auditory function in mice and humans. J Neurosci. 2008; 28:7350–8. [PubMed: 18632939]

Everett LA, Belyantseva IA, Noben-Trauth K, Cantos R, Chen A, Thakkar SI, Hoogstraten-Miller SL, Kachar B, Wu DK, Green ED. Targeted disruption of mouse Pds provides insight about the inner-ear defects encountered in Pendred syndrome. Hum Mol Genet. 2001; 10:153–61. [PubMed: 11152663]

Failli V, Bachy I, Retaux S. Expression of the LIM-homeodomain gene Lmx1a (dreher) during development of the mouse nervous system. Mech Dev. 2002; 118:225–8. [PubMed: 12351192]

Fekete DM, Wu DK. Revisiting cell fate specification in the inner ear. Curr Opin Neurobiol. 2002; 12:35–42. [PubMed: 11861162]

Giraldez F. Regionalized organizing activity of the neural tube revealed by the regulation of lmx1 in the otic vesicle. Dev Biol. 1998; 203:189–200. [PubMed: 9806783]

Hatch EP, Noyes CA, Wang X, Wright TJ, Mansour SL. Fgf3 is required for dorsal patterning and morphogenesis of the inner ear epithelium. Development. 2007; 134:3615–25. [PubMed: 17855431]

Hobert O, Westphal H. Functions of LIM-homeobox genes. Trends Genet. 2000; 16:75–83. [PubMed: 10652534]

Huang M, Sage C, Li H, Xiang M, Heller S, Chen ZY. Diverse expression patterns of LIM-homeodomain transcription factors (LIM-HDs) in mammalian inner ear development. Dev Dyn. 2008; 237:3305–3312. [PubMed: 18942141]

Karet FE, Finberg KE, Nelson RD, Nayir A, Mocan H, Sanjad SA, Rodriguez-Soriano J, Santos F, Cremers CW, Di Pietro A, Hoffbrand BI, Winiarski J, Bakkaloglu A, Ozen S, Dusunsel R, Goodyer P, Hulton SA, Wu DK, Skvorak AB, Morton CC, Cunningham MJ, Jha V, Lifton RP. Mutations in the gene encoding B1 subunit of H+-ATPase cause renal tubular acidosis with sensorineural deafness. Nat Genet. 1999; 21:84–90. [PubMed: 9916796]

Kelley MW. Regulation of cell fate in the sensory epithelia of the inner ear. Nat Rev Neurosci. 2006; 7:837–49. [PubMed: 17053809]

Koundakjian EJ, Appler JL, Goodrich LV. Auditory neurons make stereotyped wiring decisions before maturation of their targets. J Neurosci. 2007; 27:14078–88. [PubMed: 18094247]

Lawoko-Kerali G, Rivolta MN, Lawlor P, Cacciabue-Rivolta DI, Langton-Hewer C, van Doorninck JH, Holley MC. GATA3 and NeuroD distinguish auditory and vestibular neurons during development of the mammalian inner ear. Mech Dev. 2004; 121:287–99. [PubMed: 15003631]

Lin Z, Cantos R, Patente M, Wu DK. Gbx2 is required for the morphogenesis of the mouse inner ear: a downstream candidate of hindbrain signaling. Development. 2005; 132:2309–18. [PubMed: 15829521]

Liu M, Pereira FA, Price SD, Chu MJ, Shope C, Himes D, Eatock RA, Brownell WE, Lysakowski A, Tsai MJ. Essential role of BETA2/NeuroD1 in development of the vestibular and auditory systems. Genes Dev. 2000; 14:2839–54. [PubMed: 11090132]

Mann RS, Carroll SB. Molecular mechanisms of selector gene function and evolution. Curr Opin Genet Dev. 2002; 12:592–600. [PubMed: 12200165]

Mansour SL, Goddard JM, Capecchi MR. Mice homozygous for a targeted disruption of the proto-oncogene int-2 have developmental defects in the tail and inner ear. Development. 1993; 117:13–28. [PubMed: 8223243]

Manzanares M, Trainor PA, Ariza-McNaughton L, Nonchev S, Krumlauf R. Dorsal patterning defects in the hindbrain, roof plate and skeleton in the dreher (dr(J)) mouse mutant. Mech Dev. 2000; 94:147–56. [PubMed: 10842066]

Matei V, Pauley S, Kaing S, Rowitch D, Beisel KW, Morris K, Feng F, Jones K, Lee J, Fritzsch B. Smaller inner ear sensory epithelia in Neurog 1 null mice are related to earlier hair cell cycle exit. Dev Dyn. 2005; 234:633–50. [PubMed: 16145671]

McKay IJ, Lewis J, Lumsden A. The role of FGF-3 in early inner ear development: an analysis in normal and kreisler mutant mice. Dev Biol. 1996; 174:370–8. [PubMed: 8631508]

Merlo GR, Paleari L, Mantero S, Zerega B, Adamska M, Rinkwitz S, Bober E, Levi G. The Dlx5 homeobox gene is essential for vestibular morphogenesis in the mouse embryo through a BMP4-mediated pathway. Dev Biol. 2002; 248:157–69. [PubMed: 12142028]

Milan M, Cohen SM. Notch signaling is not sufficient to define the affinity boundary between dorsal and ventral compartments. Mol Cell. 1999; 4:1073–8. [PubMed: 10635331]

Milan M, Cohen SM. A re-evaluation of the contributions of Apterous and Notch to the dorsoventral lineage restriction boundary in the Drosophila wing. Development. 2003; 130:553–62. [PubMed: 12490561]

Millen KJ, Millonig JH, Hatten ME. Roof plate and dorsal spinal cord d11 interneuron development in the *dreher* mutant mouse. Dev Biol. 2004; 270:382–392. [PubMed: 15183721]

Millonig JH, Millen KJ, Hatten ME. The mouse Dreher gene Lmx1a controls formation of the roof plate in the vertebrate CNS. Nature. 2000; 403:764–9. [PubMed: 10693804]

Morsli H, Choo D, Ryan A, Johnson R, Wu DK. Development of the mouse inner ear and origin of its sensory organs. J Neurosci. 1998; 18:3327–35. [PubMed: 9547240]

Morsli H, Tuorto F, Choo D, Postiglione MP, Simeone A, Wu DK. Otx1 and Otx2 activities are required for the normal development of the mouse inner ear. Development. 1999; 126:2335–43. [PubMed: 10225993]

Nichols DH, Pauley S, Jahan I, Beisel KW, Millen KJ, Fritzsch B. Lmx1a is required for segregation of sensory epithelia and normal ear histogenesis and morphogenesis. Cell Tissue Res. 2008; 334:339–58. [PubMed: 18985389]

Pearse RV 2nd, Scherz PJ, Campbell JK, Tabin CJ. A cellular lineage analysis of the chick limb bud. Dev Biol. 2007; 310:388–400. [PubMed: 17888899]

Ponnio T, Burton Q, Pereira FA, Wu DK, Conneely OM. The nuclear receptor Nor-1 is essential for proliferation of the semicircular canals of the mouse inner ear. Mol Cell Biol. 2002; 22:935–45. [PubMed: 11784868]

Pressman CL, Chen H, Johnson RL. LMX1B, a LIM homeodomain class transcription factor, is necessary for normal development of multiple tissues in the anterior segment of the murine eye. Genesis. 2000; 26:15–25. [PubMed: 10660670]

Raft S, Koundakjian EJ, Quinones H, Jayasena CS, Goodrich LV, Johnson JE, Segil N, Groves AK. Cross-regulation of Ngn1 and Math1 coordinates the production of neurons and sensory hair cells during inner ear development. Development. 2007; 134:4405–15. [PubMed: 18039969]

Riccomagno MM, Martinu L, Mulheisen M, Wu DK, Epstein DJ. Specification of the mammalian cochlea is dependent on Sonic hedgehog. Genes Dev. 2002; 16:2365–78. [PubMed: 12231626]

Riccomagno MM, Takada S, Epstein DJ. Wnt-dependent regulation of inner ear morphogenesis is balanced by the opposing and supporting roles of Shh. Genes Dev. 2005; 19:1612–23. [PubMed: 15961523]

Riddle RD, Ensini M, Nelson C, Tsuchida T, Jessell TM, Tabin C. Induction of the LIM homeobox gene Lmx1 by WNT7a establishes dorsoventral pattern in the vertebrate limb. Cell. 1995; 83:631–40. [PubMed: 7585966]

Salminen M, Meyer BI, Bober E, Gruss P. Netrin 1 is required for semicircular canal formation in the mouse inner ear. Development. 2000; 127:13–22. [PubMed: 10654596]

Satoh T, Fekete DM. Retroviral vectors to study cell differentiation. Front Biosci. 2003; 8:d183–92. [PubMed: 12456350]

Steel KP, Davidson DR, Jackson IJ. TRP-2/DT, a new early melanoblast marker, shows that steel growth factor (c-kit ligand) is a survival factor. Development. 1992; 115:1111–9. [PubMed: 1280558]

Stevens CB, Davies AL, Battista S, Lewis JH, Fekete DM. Forced activation of Wnt signaling alters morphogenesis and sensory organ identity in the chicken inner ear. Dev Biol. 2003; 261:149–64. [PubMed: 12941626]

Vogel A, Rodriguez C, Warnken W, Izpisua Belmonte JC. Dorsal cell fate specified by chick Lmx1 during vertebrate limb development. Nature. 1995; 378:716–20. [PubMed: 7501017]

Wahlsten D, Lyons JP, Zagaja W. Shaker short-tail, a spontaneous neurological mutant in the mouse. The Journal of Heredity. 1983; 74:421–425.

Williams JA, Paddock SW, Carroll SB. Pattern formation in a secondary field: a hierarchy of regulatory genes subdivides the developing Drosophila wing disc into discrete subregions. Development. 1993; 117:571–84. [PubMed: 8330528]

Zopf, D.; Kondo, T.; Aloor, H.; Hashino, E. Spatio-temporal expression patterns of Tlx3 in the developing inner ear. 32nd MidWinter Meeting for Association for Research in Otolaryngology; 2007. Abstract #88

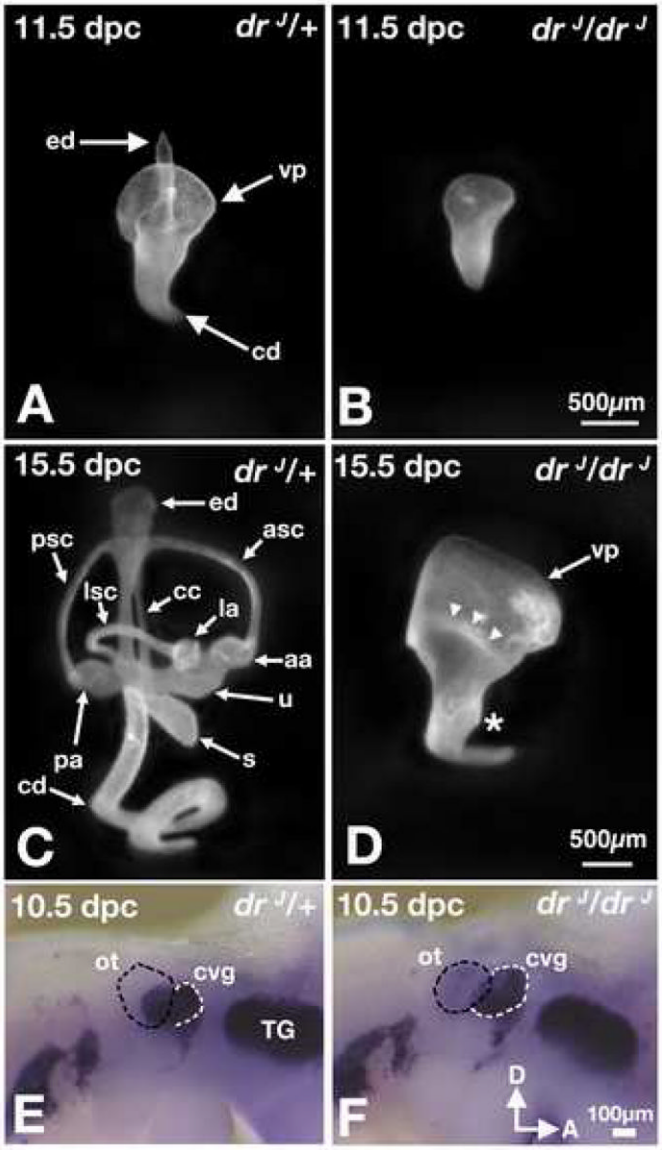

Fig. 1. Paint-filled and whole-mount inner ears of dr^J/dr^J mutants

Lateral views of $dr^J/+$ (A,C) and dr^J/dr^J (B,D) inner ears. (A,B) At 11.5 dpc, inner ears of dr^J/dr^J mutants lack the endolymphatic duct. The canal pouches are smaller in size and the cochlear duct has limited extension. (C,D) At 15.5 dpc, the morphologies of dr^J/dr^J inner ears remain rudimentary compared to those in $dr^J/+$ embryos. The vertical (vp) and lateral (arrowheads) canal pouches show no sign of resorption, and extension of the cochlear duct is limited. Asterisk indicates the rudimentary saccule. (E,F) Whole-mount $dr^J/+$ (E) dr^J/dr^J (F) embryos probed for *NeuroD* transcripts. An increase in the size of CVG (white outline) is apparent adjacent to the dr^J/dr^J otocyst (black outline), showing *NeuroD*-positive neuroblasts within the otic epithelium that have not yet delaminated and are not part of the CVG. aa, anterior ampulla; asc, anterior semicircular canal; cd, cochlear duct; ed, endolymphatic duct; la, lateral ampulla; pa, posterior ampulla; ot, otocyst; psc, posterior semicircular canal; s, saccule; TG, trigeminal ganglion; u, utricle; vp, vertical canal pouch.

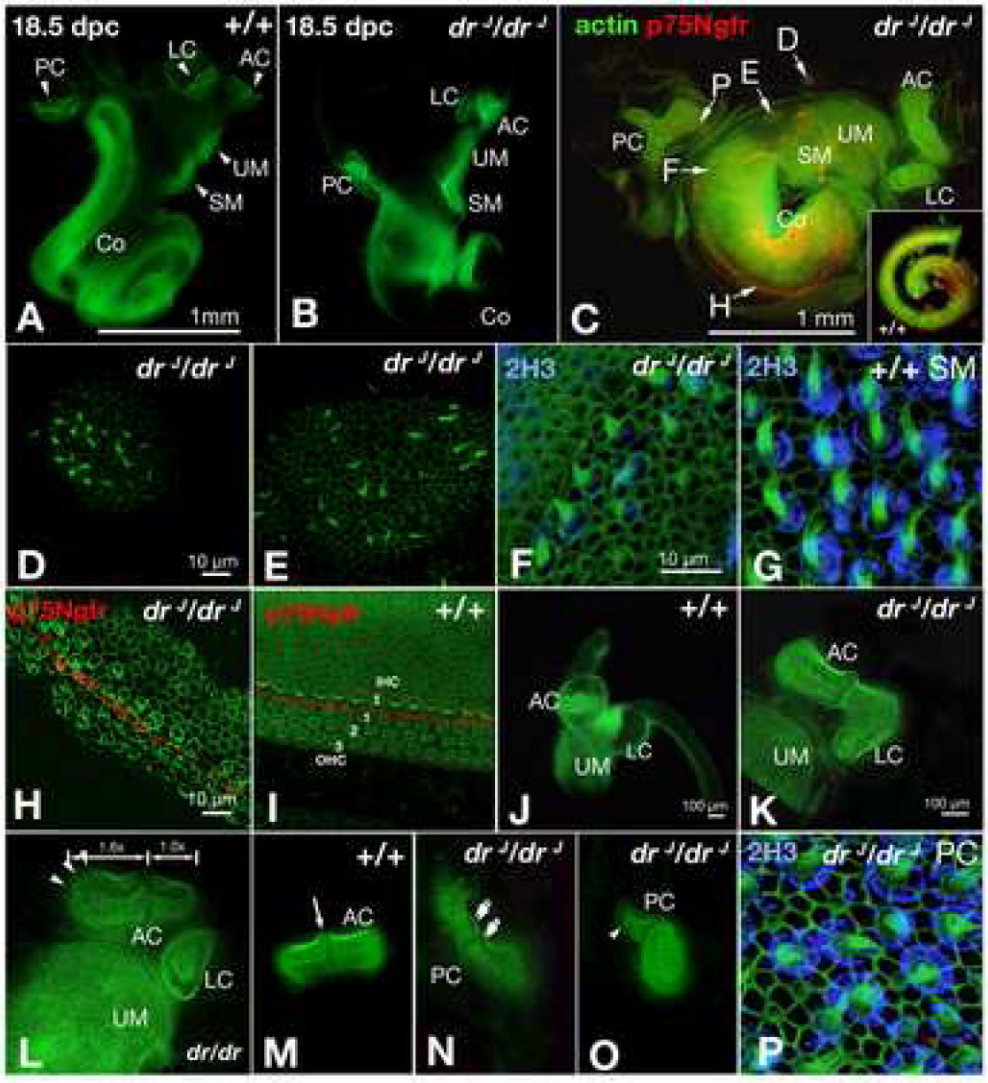

Fig. 2. Abnormal sensory organs in dr^J/dr^J inner ears

(A-P) Whole-mount sensory epithelia labeled with FITC-phalloidin. Some specimens are double-labeled with anti-2H3 for neurofilament (F,G,P) or anti-p75Ngfr for pillar cells (C,H,I). (A,B) Sensory organs are housed in separate chambers in wildtype inner ears, but they are located within a common chamber in dr^J/dr^J mutants. (C) Image of a flattened dr^J/dr^J inner ear. The cristae are abnormal in shape, the cochlear duct only has a ¾ turn, and p75Ngfr labeling is absent in the basal turn (F). Inset shows normal p75Ngfr labeling in a wildtype cochlear duct. (D,E,F,H,P) are higher power views of specific regions in (C). (D,E) Ectopic sensory patches located adjacent to the maculae of the utricle and saccule (UM, SM). (F) Presence of hair cells in the p75Ngfr-negative, basal turn area of dr^J/dr^J cochlear duct. The hair bundles resemble those in a normal macula, but the cell bodies are not surrounded by 2H3-positive calyxes as in a normal macula (G). (H) Middle turn of dr^J/dr^J cochlear duct showing disorganized hair cells that are separated by a row of p75Ngfr-positive pillar cells. (I) Middle turn of wildtype cochlea showing three rows of outer hair cells and one row of inner hair cells, separated by a row of p75Ngfr labeling. (J) Wildtype inner ear showing the anterior crista, lateral crista, and utricular macula in separate chambers. (K) Fusion of the anterior and lateral cristae in dr^J/dr^J mutants. (L) Asymmetrical

shape of the anterior crista in dr^J/dr^J. The medial half of the AC is 1.6 times longer than the lateral half. (M) Symmetrical shape of AC in wildtype. (N,O) Abnormal posterior cristae in dr^J/dr^J mutants with one consisting of two cruciata (double arrows) and another with asymmetrical halves (arrowhead). (P) Posterior crista of dr^J/dr^J showing normal hair bundles and calyxes. AC, anterior crista; LC, lateral crista; PC, posterior crista; UM, utricular macula; SM, saccular macula; Co, cochlea. Scale bars: (A,B);(D,E);(F,G,P);(H,I);(K-O).

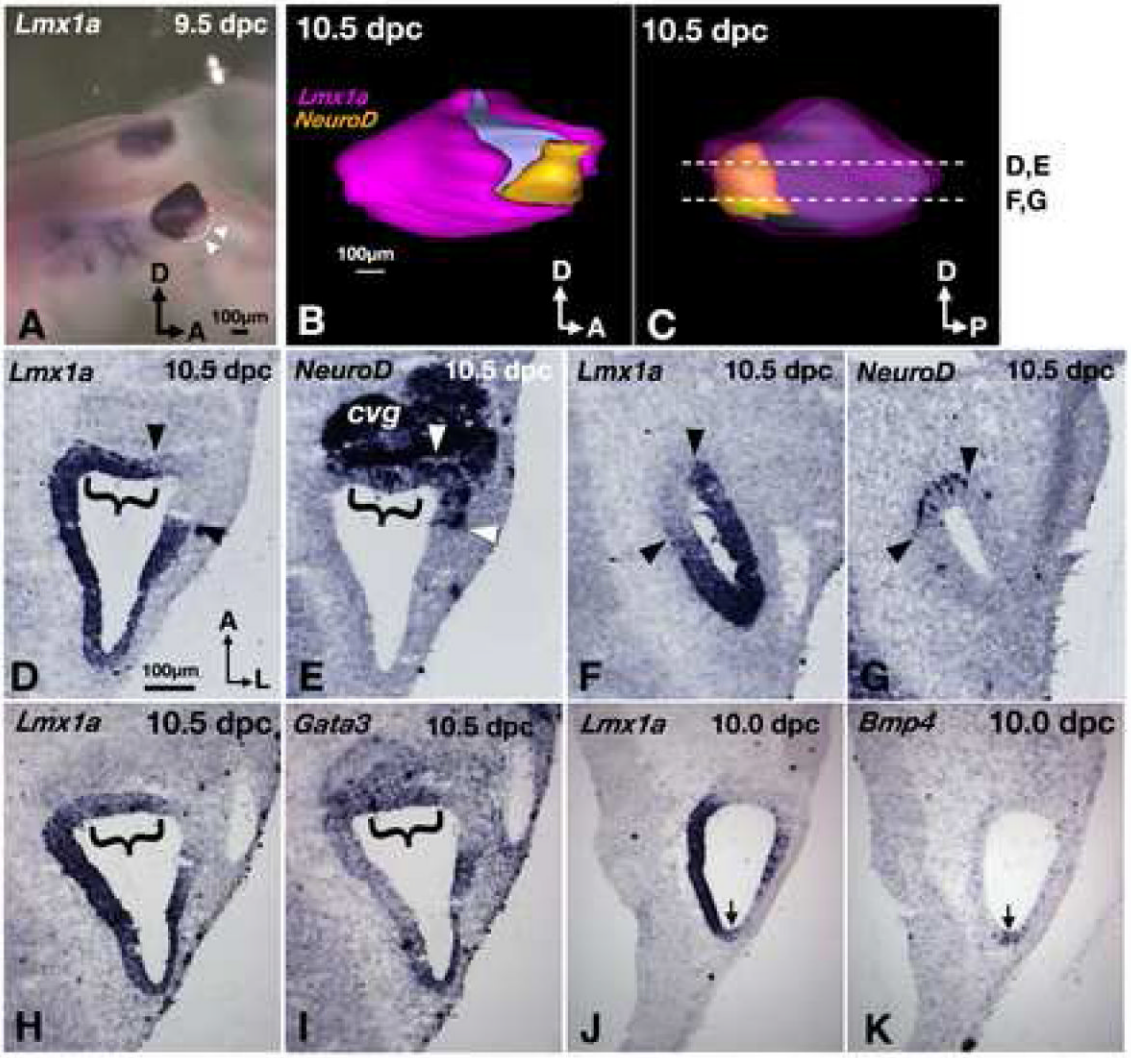

Fig. 3. *Lmx1a* expression influences neural subtype specification

(A) *Lmx1a* expression in a whole-mount embryo. *Lmx1a* is not expressed in the antero-ventral region of the otocyst (arrowheads). (B) Lateral and (C) medial views of a 3-D reconstructed inner ear showing the relationships of *Lmx1a* (pink) and *NeuroD* (yellow) expression domains. The pink in (C) is rendered transparent to reveal the yellow area underneath. Asterisk indicates the neurogenic region that is devoid of *Lmx1a* expression. (D-G) Representative sections from ear shown in (B) and (C). Brackets indicate the neurogenic regions that do express *Lmx1a*. Arrowheads mark the neurogenic regions that do not express *Lmx1a*. (H,I) adjacent sections probed for *Lmx1a* (H) and *Gata3* (I). (J,K) adjacent sections probed for *Lmx1a* (J), and *Bmp4* (K), showing *Lmx1a* expression in the *Bmp4*-positive posterior crista (arrows). Sections are rotated 90° clockwise from orientation in (C). Orientation and scale bar in D apply to E–K.

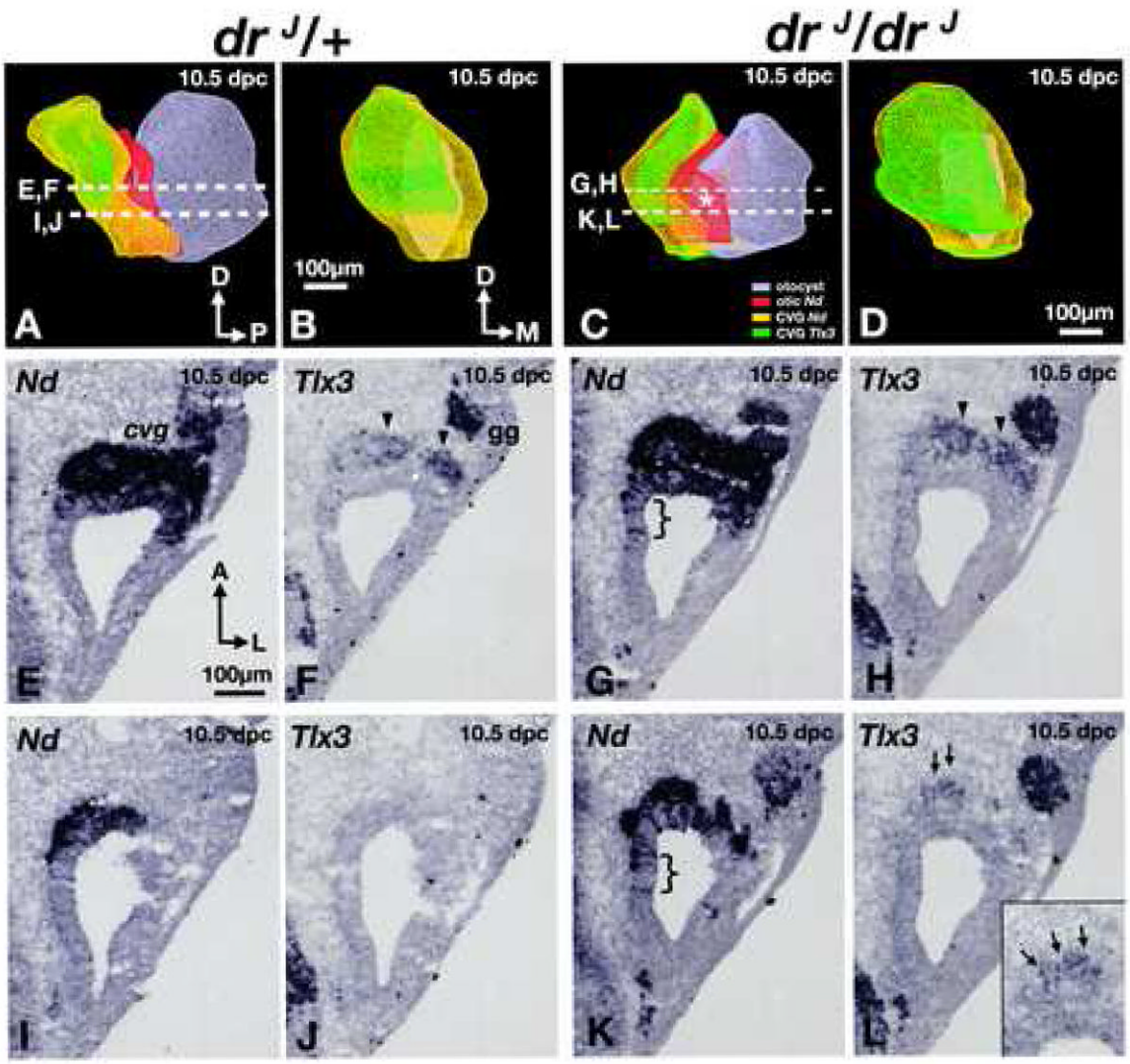

Fig. 4. Ganglion malformations in dr^J/dr^J mutants

(A,C) Antero-medial views of 3-D reconstructed, right inner ears (grey) of (A) heterozygous and (C) homozygous dr^J/dr^J mutants. *NeuroD* expression within the otocyst is red, and expression of *NeuroD* and *Tlx3* in the CVG are yellow and green, respectively. Asterisk represents a medial expansion of the *NeuroD* domain in the *dreher* otocyst. (B,D) Anterior views of the CVG in (A) and (C), respectively. (E,F) and (I,J) are representative sections from the dr^J/+ specimen shown in (A). Comparable sections from the dr^J/dr^J specimen in (C) are shown in (G,H) and (K,L). (E-H) At this level, there is an expansion of the neurogenic domain (G; bracket) and more *Tlx3* expression in the CVG of dr^J/dr^J compared to dr^J/+ (H; arrowheads). (I-J) Slightly ventral, where there is only residual neurogenic domain that is *Tlx3* negative in dr^J/+, there is a broader neurogenic domain in dr^J/dr^J mutants (K; bracket) and some *Tlx3*-positive neuroblasts can be detected (L; arrows; inset). Sections are rotated 90° clockwise from orientation in (A or C). gg, geniculate ganglion. Orientation and scale bar in E apply to F-L.

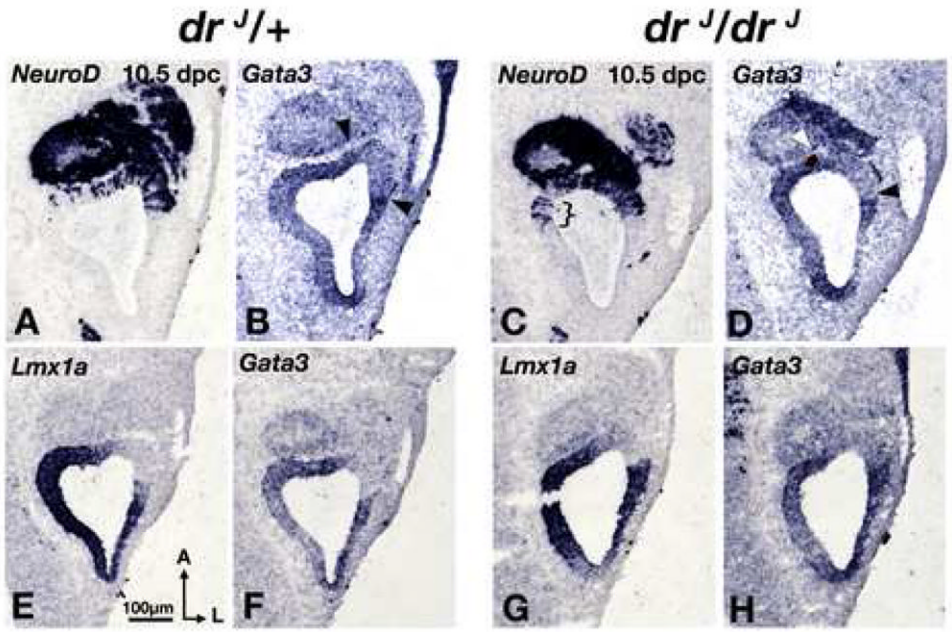

Fig. 5. *Gata3* expression domain is unchanged in dr^J/dr^J mutants

(A,B) and (C,D) are comparable midsections of dr^J/+ and dr^J/dr^J otocysts, respectively. There is no obvious difference in *Gata3* expression domains between the two genotypes. However, there is a clear medial expansion of *NeuroD* expression in the dr^J/dr^J mutant (C; bracket). (E,F) and (G,H) are comparable midsections of dr^J/+ and dr^J/dr^J otocysts, respectively. There is no difference in the expression pattern of *Lmx1a* or *Gata3* between the two genotypes. Sections chosen in this figure are at comparable levels to those shown in Fig. 4 (E-H).

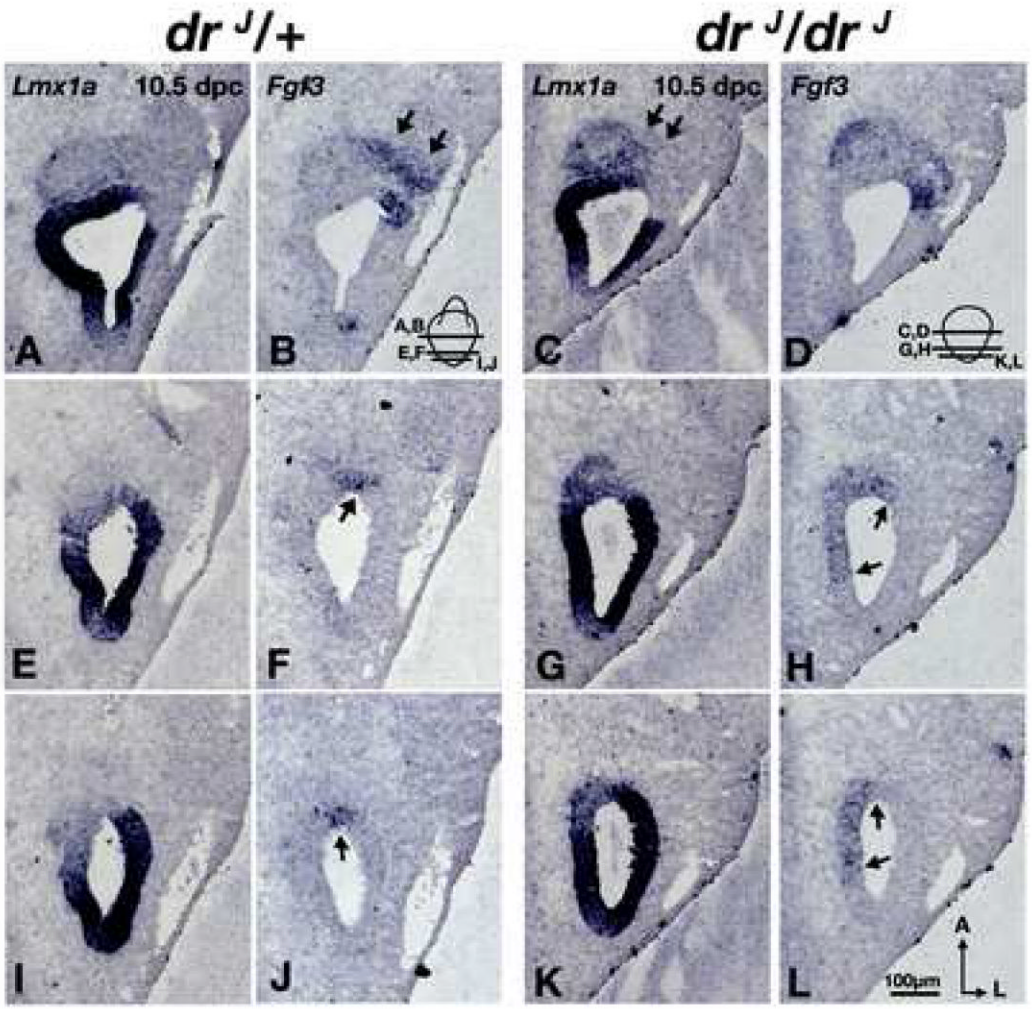

Fig. 6. Expansion of the vestibular neurogenic region in dr^J/dr^J mutants

(A,B) and (C,D) are comparable midsections of dr^J/+ and dr^J/dr^J otocysts, respectively. There is no obvious difference between dr^J/+ and dr^J/dr^J in their *Lmx1a* (A,C) and *Fgf3* (B,D) expression domains except there is more *Lmx1a* expression in delaminated neuroblasts of dr^J/dr^J mutants (C; arrows). At a more ventral level (E-L), *Fgf3* expression is expanded medially in dr^J/dr^J mutants (H,L; arrows). Orientation and scale bar apply to all.

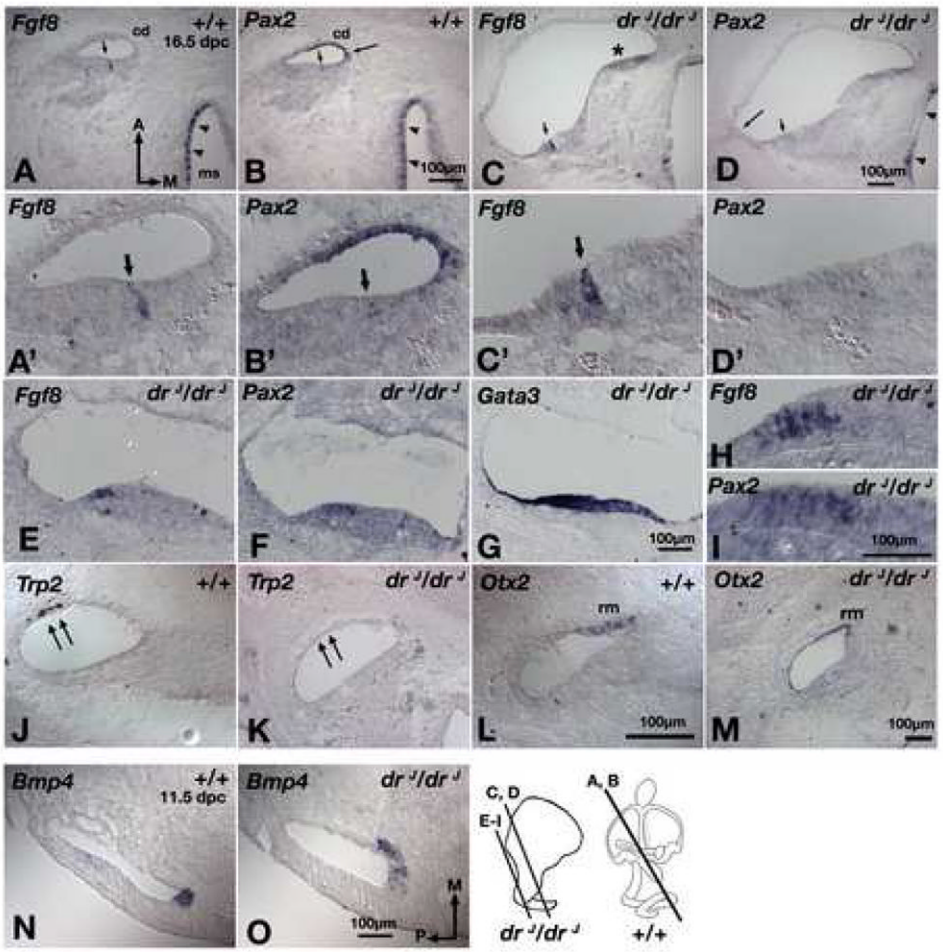

Fig. 7. Abnormal gene expression patterns in the cochlear duct and cristae of dr^J/dr^J mutants

(A,B) Adjacent sections of wildtype inner ears showing *Fgf8* (A) is expressed in the inner hair cells of the organ of Corti (arrow) and hair cells of the macula of the saccule (ms; arrowheads). *Pax2* (B) is expressed in the stria vascularis (long arrow), hair cells of the vestibule (arrowheads), but expression in the hair cells of the organ of Corti is barely detectable (short arrow). (C,D) Adjacent sections of the apical region of dr^J/dr^J cochlear duct showing *Fgf8* (C) is expressed in the inner hair cells of the organ of Corti, but *Pax2* (D) is in neither the stria vascularis (long arrow) nor sensory hair cells (short arrow). Asterisk indicates an area where the tissue is folded. (A'-D') Higher magnification of sections shown in (A-D). (E,F,G) Adjacent sections of the basal region of the dr^J/dr^J cochlear duct showing high numbers of hair cells expressing *Fgf8* (E) and *Pax2* (F) in a *Gata3*-positive, cochlear region (G). (H,I) Higher magnification of sections shown in (E) and (F), respectively. (J,L) In wildtype cochlear duct, *Trp2* (J) and *Otx2* (L) are expressed in the stria vascularis (double arrows) and Reissner's membrane (rm), respectively. In dr^J/dr^J cochlear duct, *Pax2* (D, long arrow) and *Trp2* (K) in the stria vascularis are not detected, but *Otx2* expression in the Reissner's membrane is evident (M). (N,O) *Bmp4* expression in the presumptive anterior crista is expanded medially in dr^J/dr^J inner ears (O) compared to wildtype (N). cd, cochlear duct. Scale bars: (A,B);(C,D);(E-G);(H,I);(J-L);(N,O)

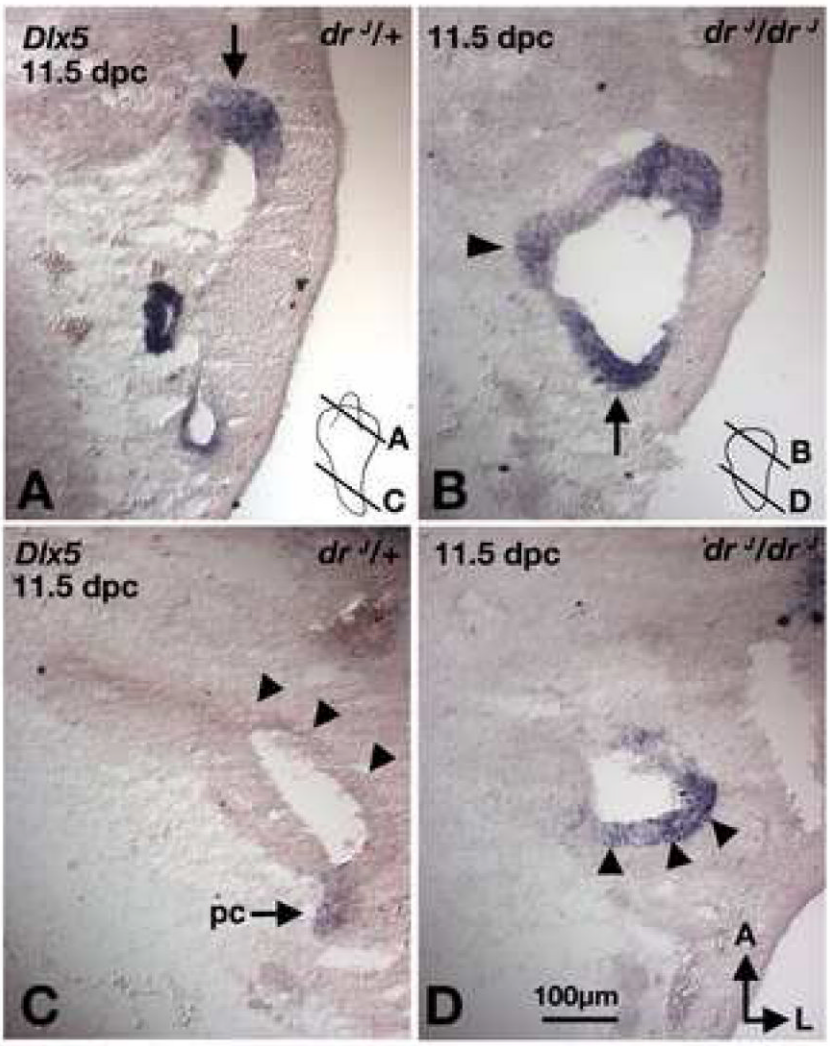

Fig. 8. Expression patterns of *Dlx5* in dr^J/dr^J mutants

Sections taken from comparable regions of $dr^J/+$ (A,C) and dr^J/dr^J (B,D) inner ears. (A,B) In the dorsal otic region, *Dlx5* expression is located in the rim of the canal pouches in both $dr^J/+$ and dr^J/dr^J ears (arrows). (C,D) *Dlx5* is only expressed in the lateral side of the cochlear duct region in dr^J/dr^J but not $dr^J/+$ ears (arrowheads). Orientation and scale bar apply to all.

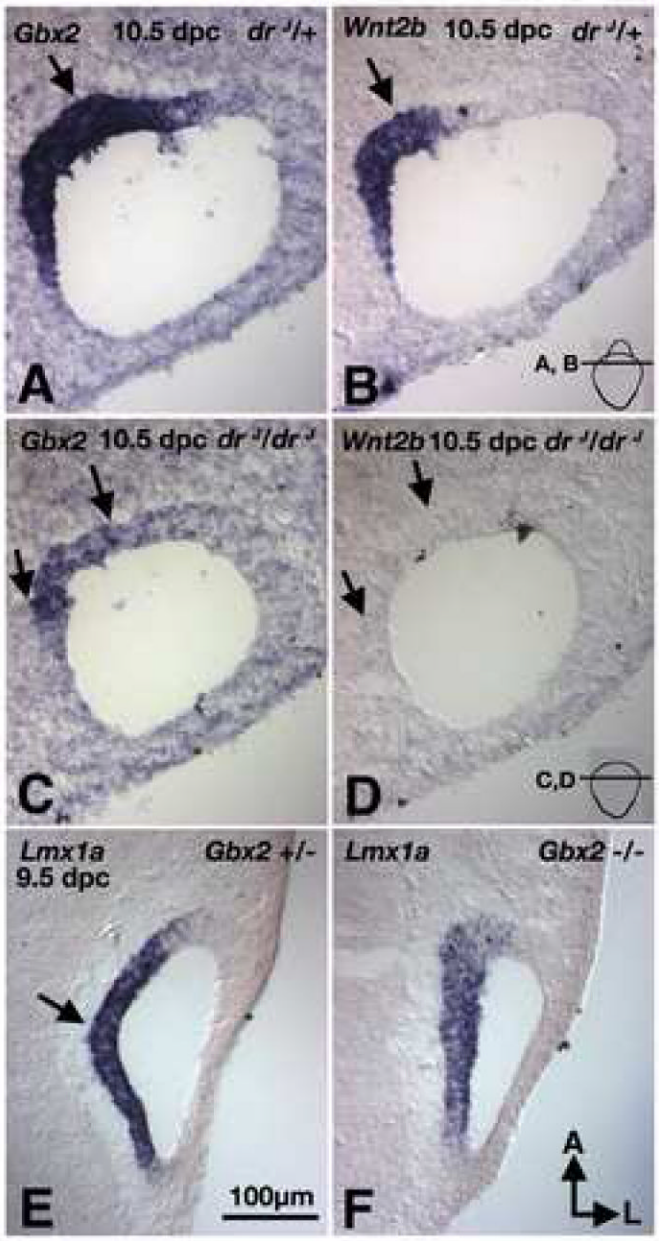

Fig. 9. Gene expression analyses of the endolymphatic duct phenotype in dr^J/dr^J and *Gbx2*-/- mutants

(A,B) Adjacent sections of dr^J/+ inner ears probed for *Gbx2* (A) and *Wnt2b* (B) transcripts. *Gbx2* and *Wnt2b* are co-expressed in the base of the endolymphatic duct region (arrow). (C,D) Adjacent sections of dr^J/dr^J inner ears from a comparable region as (A,B) and probed for *Gbx2* (C) and *Wnt2b* (D) transcripts. *Gbx2* expression is present in dr^J/dr^J mutants but not *Wnt2b*. (E,F) In *Gbx2* null embryos *Lmx1a* is present in the medial region (F), similar to the *Gbx2* +/- embryos (E). Orientation and scale bar apply to all.

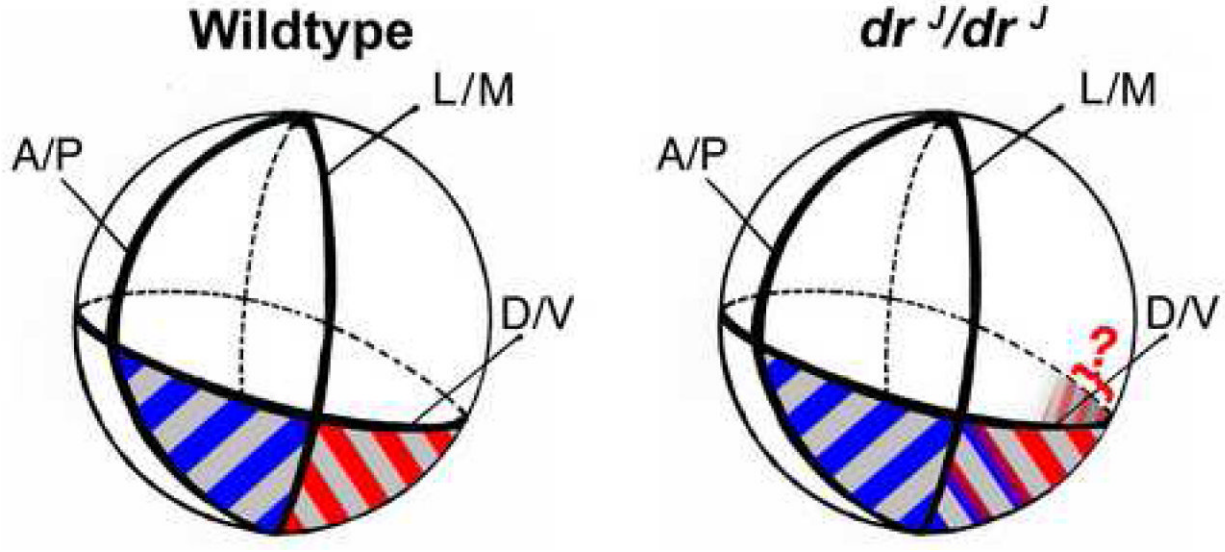

Fig. 10. Lmx1a maintains specified domains

The globes represent the developing otocyst in wildtype and dr^J/dr^J mutants. The ventral neurogenic region is shaded gray. The ventro-lateral putative vestibular neurogenic region (blue stripes) is *Lmx1a*-negative, *Fgf3*-positive, and *Gata3*-negative. The ventro-medial, presumably auditory neurogenic region (red stripes) is *Lmx1a*-positive, *Fgf3*-negative, and *Gata3*-positive. In the developing otocysts of wildtype mice there is a distinct border between the *Fgf3* and *Lmx1a* expression domains. However, in dr^J/dr^J, non-functional Lmx1a cannot maintain the proper *Fgf3*–positive region and the *Fgf3* expression domain expands medially (blue-red gradient). *Lmx1a* expression domain does not change, but the ventro-medial neurogenic region (gray shading in dr^J/dr^J) is expanded posteriorly in the mutant otocyst. Because *Gata3* is normally expressed at low levels in the medial otic epithelium, it is unclear whether the *Gata3* domain is expanded in that region of dr^J/dr^J otocyst (red question mark).